Tetrahedron Letters 49 (2008) 4949–4952

Contents lists available at ScienceDirect

Tetrahedron Letters

journal homepage: www.elsevier.com/locate/tetlet

Divergent synthesis and optoelectronic properties of oligodiacetylene building blocks

Gregor S. Pilzak, Barend van Lagen, Ernst J. R. Sudhölter †, Han Zuilhof *

Laboratory of Organic Chemistry, Wageningen University, Dreijenplein 8, 6703 HB Wageningen, The Netherlands

ARTICLE INFO

Article history:
Received 24 March 2008
Revised 20 May 2008
Accepted 28 May 2008
Available online 3 June 2008

ABSTRACT

A new and divergent synthetic route to oligodiacetylene (ODA) building blocks has been developed via Sonogashira reactions under a reductive atmosphere. These central building blocks provide a new way for rapid preparation of long ODAs. In addition, we report on their optoelectronic properties which are dependent on their end cap. Finally, the formation of their radical cations, and their optical properties and reactivity towards nucleophiles are investigated.

© 2008 Elsevier Ltd. All rights reserved.

The development of precisely defined π-conjugated oligomers has developed significantly in the last decade, since such monodisperse oligomers function as model systems to determine the evolution of the optical and electronic properties of the corresponding polymers[1–3] Recently, our systematic studies of the optical properties of highly soluble all-*trans* oligodiacetylenes (ODA)[4] and homo-oligodiacetylenes[5] have provided new information about the relationship between oligomer length (up to 8.2 nm) and the optoelectronic properties of polydiacetylene-related materials. This made it possible to distinguish intra- and intermolecular effects on the light absorption of these extended conjugated systems. However, the iterative synthesis of these materials is a rather time-consuming process, in which the oligomer backbone is extended with only one monomeric unit per elongation cycle. This chain extension could be substantially speeded up by using a central building block to couple two oligomers in just one elongation step. Moreover, such a building block should be designed in such a way that it does not alter the structure of the ODA backbone and can be implemented easily in existing ODA syntheses, to provide a new and fast way of preparing nanometer-sized ODAs.

In this study, a synthesis is presented of trimeric and monomeric central building blocks **1** and **2** for oligodiacetylene syntheses (Fig. 1). In addition, we have studied the influence of the end caps on the optical properties of the oligomer backbone, and, for the first time, the optoelectronic properties of the corresponding radical cations.

The ODA building block **1** was prepared via a divergent approach as illustrated in Figure 2. The ODA backbone bears two asymmetrical alkyl chains. These provide, firstly, steric hindrance,

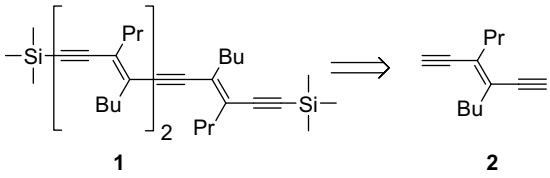

Figure 1. Retrosynthesis of the oligodiacetylenes under present study.

and therefore hamper the interchain π–π stacking. Secondly, their structural asymmetry is highly beneficial, as this improves substantially the solubility. Finally, the TMS end caps can be removed rapidly and quantitatively under mild, alkaline conditions yielding a terminal *bis*-acetylene that can be used as the central unit in a divergent synthesis of enediyne-containing materials. The synthesis of the *trans*-iodoenyne **3** is described elsewhere.[4] The mild coupling of the terminal acetylene **4** with **3** was performed via a Sonogashira reaction yielding ene–diyne **5** in 95% isolated yield.[6] The alkaline protodesilylation of **5** proceeds quantitatively, and results in ene–diyne **2** bearing two terminal acetylene groups. The following divergent elongation step consists of catalytic coupling of **2** with two ODA blocks **3** under a diluted hydrogen atmosphere. This was done to prevent oxidation of the palladium catalyst, which would otherwise initiate polymerization of the terminal acetylenes.[7] Unreacted **3** was recovered quantitatively after the elongation step, which allowed the use of a large excess of this material. This elongation process adds eight conjugated C atoms to the ODA chain in a single reaction step. The catalytic coupling of *trans*-iodoenyne **3** to building block **1** can be repeated in this fashion to yield long-chain ODAs, or related materials.[8]

The ground state absorption and fluorescence emission of the newly synthesized building blocks **5** and **1** were recorded in *n*-hexane. In order to study the influence of the end caps on the optoelectronic properties of the ODAs, a novel oligomer **6** was synthesized

* Corresponding author. Tel.: +31 317 482367; fax: +31 317 484914.
E-mail address: Han.Zuilhof@wur.nl (H. Zuilhof).
† Present address: Delft University of Technology, DelftChemTech, Laboratory of Nano-organic chemistry, Julianalaan 136, 2628 BL Delft, The Netherlands.

0040-4039/$ - see front matter © 2008 Elsevier Ltd. All rights reserved.
doi:10.1016/j.tetlet.2008.05.135

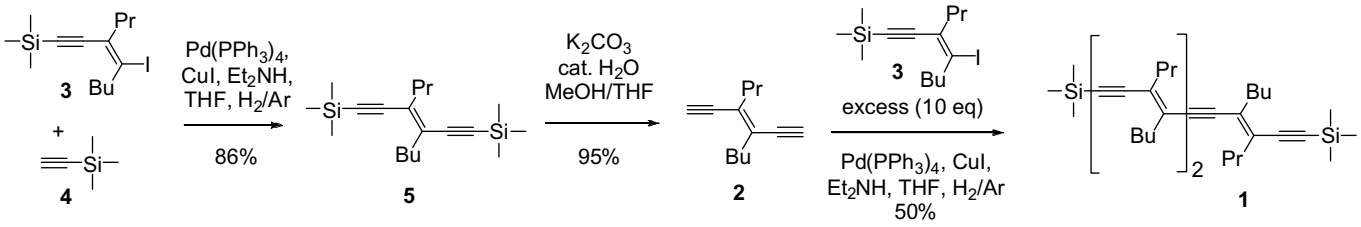

Figure 2. Divergent synthesis of oligodiacetylene building blocks.

having methyl and *t*-CMe_2OMe end caps (Fig. 3).[9] The absorption and emission spectra of these ODAs are shown in Figure 3 together with the literature data of previously synthesized ene–diyne **7** and ODA **8** with TMS and *t*-CMe_2OMe end caps.[4] The absorption spectra clearly show a bathochromic shift and an increase of the absorption with chain elongation. The ε_{max} increases by 78% going from **5** with the conjugation length (CL) of 3 conjugated double and triple bonds, to **1** (CL = 7). The optical properties of ODA building blocks are dominated by the C_{2h} symmetry that is present in fully stretched, planar oligomers, and their absorption spectrum is associated with the S_2 (1^1B_u)←S_0 (1^1A_g) transition.[4,10,11] The influence of the end cap on the absorption is small but clear: a red-shift of 10 nm (0.17 eV) is induced when the less electron-donating Me-group in **6** is exchanged for a TMS-group in **7**. Analogous but smaller effects were observed when the *t*-CMe_2OMe group was exchanged for a TMS group, that is, 5 nm (0.09 eV) and 4 nm (0.03 eV) for ODAs with CL of 3 and 7, respectively. Similar red-shifting of the absorption is reported for ODAs[11] and oligotriacetylenes[12] upon introduction of electron-donating end groups, whilst blue-shifts are observed when an electron-withdrawing end cap is added to carotenoid derivatives[13] and distyryl-benzenes.[14] The extinction coefficient is also affected by the choice of the end caps. The TMS-end capped ODAs show higher absorptions in *n*-hexane compared to ODAs with poor electron-donating end groups. There is a substantial difference in ε_{max} of ~30% between the oligomers with two symmetrical end groups **1** and **5** compared to **7** and **8**, which have a dipole induced by the *t*-CMe_2OMe end cap. This shows that the S_2←S_0 transition for non-polar and dipole-less ODA building blocks is actually more probable in an apolar solvent. These observations are in line with the absorption increase for symmetrical homocoupled ODAs in *n*-hexane compared to 1,2-dichloroethane.[5] Specifically, building block **1** is rather fluorescent ($\Phi_f = 0.177$), keeping in mind the near-absence of fluorescence of polydiacetylenes, and the much lower quantum yield of fluorescence of **5** ($\Phi_f = 0.010$). Apparently, the extension of the conjugated system increases the density of states near the excited state level, so as to increase the rate of radiationless decay at the cost of a decreased fluorescence efficiency. As with the absorption, in comparison with a *t*-CMe_2OMe end cap, a terminal TMS group induces a red-shift of ~0.04 eV of the emission maxima. This is a direct result of the increased electron density of the backbone induced by an electron-donating end cap, and is in line with the red-shift of the λ_{max} observed for the absorption. Electron-donating end groups also result in higher quantum yields for TMS-end capped ODAs compared to oligomers with Me and *t*-CMe_2OMe substituents, specifically for **5** versus **6** and **7** (5-fold and 2.5-fold increases, respectively). The building blocks with poor electron-donating end caps show a marginal fluorescence, comparable to polydiacetylenes with typical values of $\Phi_f \ll 0.001$.[15] Picosecond time-resolved single photon counting was used to determine the fluorescence lifetimes (τ_F) of the ODA building blocks (Table 1).

The recorded τ_F matches rather closely the literature data of ODAs with the same CL,[4,11] suggesting only marginal substituent effects on the quantum yield. Fluorescence depolarization (r) of the ODA building blocks was determined by picosecond time-resolved fluorescence anisotropy measurements.[4,5,17] Since these rod-shaped oligomers possess a relatively large axial ratio, the rotation of the molecules around the longitudinal axis progresses—especially for **1** and **8**—evidently much faster compared to the rotation around the two short, perpendicular axes, that are not expected to differ significantly from each other. All the compounds under present study display mono-exponential decay kinetics $r(t)$ with an initial anisotropy value r_0 determined by the angle γ between the absorption and emission transition moment and one rotation correlation time (τ_R).[16] For all the building blocks r_0 was ~0.3, similar to that of trimeric ODAs investigated previously.[11,15,18] This indicates a small angle (~15°) between absorption and emission transition moments.

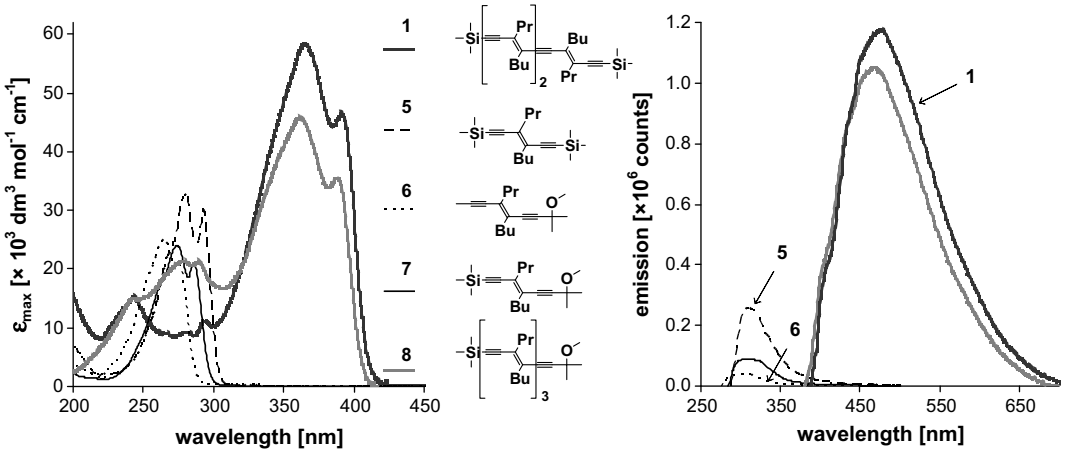

Figure 3. Absorption (left) and emission (right) spectra of the ODA building blocks in *n*-hexane at micromolar concentrations (~2×10^{-6} M).

Table 1
Absorption and emission data of ODA building blocks as millimolar solutions (2×10^{-6} M) in *n*-hexane

ODA (CL)[f]	Absorption		Emission			
	λ_{max} (nm) (eV)	ε_{max} ($\times 10^3$ dm^3 mol^{-1} cm^{-1})	λ_{max} (nm) (eV)	Fluor. quant. yield Φ_f[a,b]	τ_F[c] (ps)	τ_R[d] (ps; ±25 ps)
1 (7)	365 (3.40)	58.2	480 (2.58)	0.177	560	130
5 (3)	279 (4.44)	32.7	310 (4.00)	0.010	~30[e]	55[e]
6 (3)	264 (4.70)	25.2	305 (4.07)	0.002	~24[e]	55[e]
7 (3)	274 (4.53)	24.0	307 (4.04)	0.004	~30[e]	65[e]
8 (7)	361 (3.43)	45.7	471 (2.63)	0.159	596	155

[a] Quantum yield determined by comparison with quinine bisulfate in 0.1 M H_2SO_4: $\Phi_f = 0.535$.[16]
[b] Exp. error ±0.002.
[c] τ_F = fluorescence lifetime.
[d] τ_R = rotation correlation time.
[e] Values not accurate, as the instrument response time is 560 ps.
[f] CL = conjugation length as the number of double and triple bonds.

The use of conjugated materials in optoelectronic devices is limited frequently by the reactivity of the corresponding radical cations. We therefore employed nanosecond laser transient absorption spectroscopy to determine the optical absorption spectra of the ODA radical cations, and their reactivity towards the reactive nucleophile, nitrate.[19] Photo-induced electron transfer was effected with positively charged sensitizers [*N*-methyl acridinium hexafluoro-phosphate (NMA^+)] to obtain the ODA radical cations very efficiently, via a reduction of the back electron transfer.[5,20] An ODA solution in 1,2-dichloroethane (DCE) was prepared with NMA^+ and mesitylene as a co-sensitizer. Figure 4 shows the normalized UV–vis spectra of $\mathbf{1}^{\bullet+}$, $\mathbf{5}^{\bullet+}$ and $\mathbf{6}^{\bullet+}$ compared to the literature data of $\mathbf{7}^{\bullet+}$ and $\mathbf{8}^{\bullet+}$.[20] The calculated extinction coefficients of the ODA radical cations are $\varepsilon(\mathbf{1}^{\bullet+}) = 1.0 \times 10^3$, $\varepsilon(\mathbf{5}^{\bullet+}) = 3.2 \times 10^2$ and $\varepsilon(\mathbf{6}^{\bullet+}) = 2.0 \times 10^2$ [$M^{-1}cm^{-1}$] as determined by comparison with the extinction coefficient of quinuclidine ($\varepsilon = 2.5 \times 10^4$).[21]

We observed a red-shift of the absorption of the radical cation of **1** versus **5** that was nearly identical to that of the neutral compounds: 1.06 eV for the radical cations compared to a red-shift of 1.04 eV for the absorption in their neutral form. This is somewhat surprising, as the lower-lying excited states of radical cations usually undergo a correspondingly smaller effect of differences in conjugation. Apparently, this is nearly completely compensated for by the larger effects of electron-donating substituents on these electron-poor systems. Theoretical studies that clarify this are clearly desired. The bathochromic shift of the absorption as a result of increasing the electron density of the backbone is again visible

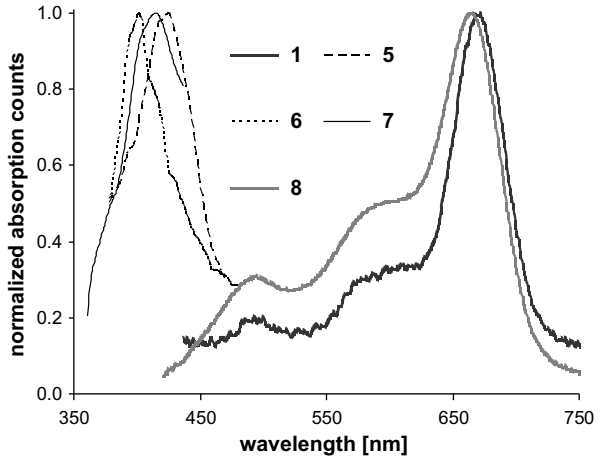

Figure 4. Transient absorption spectra of the radical cations of the ODA building blocks.

Table 2
λ_{max} and lifetimes τ of radical cations and rate constants k for nucleophilic attack of TBAN

ODA (CL)[f]	λ_{max} (nm) (eV)	τ (μs)	k_{TBAN} (M^{-1} s^{-1})
1 (7)	671 (1.85)	50	1.81×10^9
5 (3)	426 (2.91)	4	8.02×10^9
6 (3)	403 (3.08)	5	7.88×10^9
7 (3)	413 (3.00)	2	$\geqslant 1.0 \times 10^{10}$
8 (7)	666 (1.86)	52	9.91×10^8

[f] CL = conjugation length as the number of double and triple bonds.

for the radical cations, that is, introducing a TMS end cap for ODAs with CL = 3, shifts the λ_{max} of the radical cation absorption with ~0.09 eV relative to a *t*-CMe_2OMe end cap. Again, this effect is near-identical to that observed for the neutral compounds. However, this effect is smaller for longer ODAs with CL = 7, that is, 0.01 eV versus 0.03 eV for the λ_{max} red-shift of the absorption of the neutral species.

Finally, the stability of the building blocks was studied as a function of the reactivity of the corresponding radical cations with a nucleophile. We used tetrabutylammonium nitrate (TBAN), which has a high solubility in DCE that minimizes aggregate formation. The results are given in Table 2. The data summarized in Table 2 reveal that the rate constants of nucleophilic attack on the radical cation decrease by roughly one order of magnitude in going from CL = 3–7. These data suggest that significantly smaller reaction rates may be observed with extended oligomers (up to CL = 30), which would be of interest for practical applications thereof. Such studies are currently in progress in our laboratories.

In conclusion, we have developed a new and rapid divergent Sonogashira coupling for the synthesis of ODA building blocks. Absorption and emission spectra and reactivity of the corresponding radical cations confirm that the ODA with two terminal TMS groups is the most electron-rich ODA of a given conjugation length.

Acknowledgement

The authors thank the Dutch Technology Foundation STW for generous funding of this research (Project No. WPC 5740), and Dr. Jan Kroon (ECN) for helpful discussions.

References and notes

1. Müllen, K. *Pure Appl. Chem.* **1993**, *65*, 89–96.
2. Martin, R. E.; Diederich, F. *Angew. Chem., Int. Ed.* **1999**, *38*, 1350–1377.
3. Gierschner, J.; Cornil, J.; Egelhaaf, H.-J. *J. Adv. Mater.* **2007**, *19*, 173–191.
4. Pilzak, G. S.; van Lagen, B.; Hendrikx, C. C. J.; Sudhölter, E. J. R.; Zuilhof, H. *Chem. Eur. J.* **2008**, in press.
5. Pilzak, G. S.; Baggerman, J.; van Lagen, B.; Sudhölter, E. J. R.; Zuilhof, H. *Chem. Eur. J.*, Submitted for publication.

6. *Synthesis of* **5**: A mixture of (*E*)-(4-iodo-3-propyloct-3-en-1-ynyl)-trimethylsilane **3** (1.15 mmol, 0.40 g), ethynyltrimethyl-silane **4** (2.31 mmol, 0.226 g), $Pd(PPh_3)_4$ (0.06 mmol, 0.065 g), CuI (0.03 mmol, 0.005 g), and dry, degassed diethyl amine (3.0 ml) and THF (7.0 ml) was placed anaerobically in a dried 25 ml two-necked round-bottomed flask, equipped with an Ar in- and outlet, and a pressure-equalized dropping funnel under an inert atmosphere. The mixture was stirred (4 h, 30 °C), concentrated and filtered over a short silica gel column (5% Et_3N in pet-ether 40/60). Purification on reversed phase silica (ACN/EtOAc, 8.5:1.5) gave pure (*E*)-4,5-bis(2-(tri-methylsilyl)-ethynyl)non-4-ene **5** (0.99 mmol, 0.314 g, 86%) as a pale yellow oil. ^1H NMR (400 MHz, $CDCl_3$): δ 0.27 (s, 18H), 0.929 (t, 3H, J = 7.2 Hz), 0.933 (t, 3H, J = 7.2 Hz), 1.27–1.41 (m, 2H), 1.48–1.63 (m, 4H), 2.35–2.43 (m, 4H); ^{13}C NMR (100 MHz, $CDCl_3$): δ 0.0, 13.6, 13.9, 21.6, 22.1, 30.4, 34.4, 36.8, 103.8, 103.9, 104.4, 104.5, 130.5, 130.9; HRMS: obsd: 318.2196; calcd: 318.2199.
7. Elangovan, A.; Wang, Y.-H.; Ho, T.-I. *Org. Lett.* **2003**, *5*, 1841–1844.
8. *Synthesis of* **1**: (4*E*,8*E*,12*E*)-5,8,12-Tributyl-9-propyl-4,13-bis(2-(trimethylsilyl)ethynyl)hexadeca-4,8,12-trien-6,10-diyne: A solution of **5** (1 equiv) in THF/MeOH (1:1, 5 ml/mmol) H_2O (3 drops/mmol) and K_2CO_3 (2 equiv) was stirred for 3 h. After working up (Et_2O/H_2O), drying (Na_2SO_4), and concentration of the combined organic layers under vacuo, acetylene **2** was submitted as such to the chain elongation step. A mixture of **3** (10 equiv), $Pd(PPh_3)_4$ (5 mol %), CuI (2 mol %), dry, degassed Et_2NH (2 ml/mmol) and THF (5 ml/mmol) was placed anaerobically in a dried, brown two-necked round-bottomed flask, equipped with an Ar/H_2 in- and outlet, and a pressure-equalizing dropping funnel containing **2** (1 equiv). Compound **2** was added slowly (over 6 h) to the stirred mixture under a constant flow of Ar/H_2 (1:1), and stirring was continued overnight at 25 °C. Concentration, filtration over a short silica gel column (5% Et_3N in pet-ether 40/60), prepurification on reversed phase silica (ACN/EtOAc, 7/3) and purification by prep. HPLC gave pure (99.5%) **1** (50% yield), whilst unreacted iodo-diacetylene **3** was recovered quantitatively. ^1H NMR (400 MHz, $CDCl_3$): δ 0.21 (s, 18H), 0.90–0.95 (m,18H), 1.29–1.41 (m, 6H), 1.54–1.62 (m, 12H), 2.32–2.49 (m, 12H); ^{13}C NMR (100 MHz, $CDCl_3$): δ 0.0, 13.6, 13.6, 13.9, 14.0, 21.7, 21.9, 22.1, 22.3, 30.5, 30.8, 34.7, 35.0, 37.0, 37.3, 98.7, 99.1, 99.1, 103.8, 104.8, 128.8, 129.2, 129.7, 131.3; HRMS: obsd. 614.4699; calcd 614.4703.
9. *Data for* **6**: (*E*)-5-Butyl-8-methoxy-8-methyl-4-propylnona-4-en-2,6-diyne; ^1H NMR (400 MHz, $CDCl_3$): δ 0.91 (t, 3H, J = 7.2 Hz), 0.92 (t, 3H, J = 7.4 Hz), 1.26–1.42 (m, 2H), 1.47–1.62 (m, 4H), 1.49 (s, 6H), 2.04 (3H), 2.35–2.43 (m, 4H), 3.38 (s, 3H); ^{13}C NMR (100 MHz, $CDCl_3$): δ 4.7, 13.6, 14.0, 21.7, 22.0, 28.5, 30.5, 34.3, 37.3, 51.7, 71.2, 79.0, 83.9, 94.3, 99.0, 127.8, 129.8; HRMS: obsd: 260.2143; calcd: 260.2140.
10. Kohler, B. E.; Schilke, D. E. *J. Chem. Phys.* **1987**, *86*, 5214–5215.
11. Hendrikx, C. C. J.; Polhuis, M.; Pul-Hootsen, A.; Koehorst, R. B. M.; Hoek van, A.; Zuilhof, H.; Sudhölter, E. J. R. *Phys. Chem. Chem. Phys.* **2005**, *7*, 548–553.
12. Martin, R. E.; Gubler, U.; Cornil, J.; Balakina, M.; Boudon, C.; Bosshard, C.; Gisselbrecht, J.-P.; Diederich, F.; Günter, P.; Gross, M.; Brédas, J.-L. *Chem. Eur. J.* **2000**, *6*, 3622–3635.
13. Deng, Y.; Gao, G.; He, Z.; Kispert, L. D. *J. Phys. Chem. B* **2000**, *104*, 5651–5656.
14. Liu, M. S.; Jiang, X.; Liu, S.; Herguth, P.; Jen, A. K.-Y. *Macromolecules* **2002**, 3532–3538.
15. Zuilhof, H.; Barentsen, H. M.; Dijk van, M.; Sudhölter, E. J. R.; Hoofman, R. J. O. M.; Siebbeles, L. D. A.; Haas de, M. P.; Warman, J. M. Polydiacetylenes. In *Supramolecular Photosensitive and Electroactive Materials*; Nalwa, H. S., Ed.; Academic Press: San Diego, 2001; pp 339–437.
16. Lakowicz, J. R. In *Principles of Fluorescence Spectroscopy*; Kluwer Academic/Plenum Publishers, 1999; pp 420–421.
17. Kapusta, P.; Erdmann, R.; Ortmann, U.; Wahl, M. *J. Fluoresc.* **2003**, *13*, 179–183.
18. Balkowski, G. M.; Groeneveld, M.; Zhang, H.; Hendrikx, C. C. J.; Polhuis, M.; Zuilhof, H.; Buma, W. J. *J. Phys. Chem. A* **2006**, *110*, 11435–11439.
19. Gould, I. R.; Ege, D.; Moser, J. E.; Farid, S. *J. Am. Chem. Soc.* **1990**, *112*, 4290–4301.
20. Pilzak, G. S.; Fratiloiu, S.; Grozema, F.; Siebbeles, L. D. A.; Zuilhof, H. *J. Phys. Chem. A,* in preparation.
21. Dinnocenzo, J. P.; Banach, T. E. *J. Am. Chem. Soc.* **1989**, *111*, 8646–8653.